5105-76
Solar Thermal Power Systems Project
Parabolic Dish Systems Development

DOE/JPL 1060-41
Distribution Category UC-62b



# Dish Stirling Solar Receiver Combustor Test Program

C. P. Bankston
L. H. Back

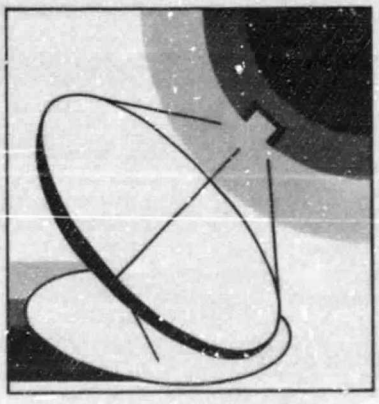


August 15, 1981

Prepared for
U.S. Department of Energy
Through an agreement with
National Aeronautics and Space Administration
by
Jet Propulsion Laboratory
California Institute of Technology
Pasadena, California

(JPL PUBLICATION 81-23)

5105-76
Solar Thermal Power Systems Project
Parabolic Dish Systems Development

DOE/JPL-1060-41
Distribution Category UC-62b

# Dish Stirling Solar Receiver Combustor Test Program

C. P. Bankston
L. H. Back

August 15, 1981

Prepared for
U.S. Department of Energy
Through an agreement with
National Aeronautics and Space Administration
by
Jet Propulsion Laboratory
California Institute of Technology
Pasadena, California

(JPL PUBLICATION 81-23)

Prepared by the Jet Propulsion Laboratory, California Institute of Technology, for the U.S. Department of Energy through an agreement with the National Aeronautics and Space Administration.

The JPL Solar Thermal Power Systems Project is sponsored by the U.S. Department of Energy and forms a part of the Solar Thermal Program to develop low-cost solar thermal and electric power plants.

## ABSTRACT

This report describes the Dish Stirling Solar Receiver (DSSR) Combustor Test Program. The overall objectives of the program were to evaluate and verify the operational and energy transfer characteristics of the DSSR combustor/heat exchanger system. The DSSR is designed to operate with fossil fuel augmentation utilizing a swirl combustor and cross flow heat exchanger consisting of a single row of 48 closely spaced tubes that are curved into a conical shape. In the present study the performance of the combustor/heat exchanger system without a Stirling engine has been studied over a range of operating conditions and output levels using water as the working fluid. Results show that the combustor may be started under cold conditions, controlled safely, and operated at a constant air/fuel ratio (~10% excess air) over the required range of firing rates. Furthermore, nondimensional heat transfer coefficients based on total heat transfer are plotted versus Reynolds number and compared with literature data taken for single rows of closely spaced tubes perpendicular to cross flow. The data show enhanced heat transfer for the present geometry and test conditions. Analysis of the results shows that the present system will meet specified thermal requirements, thus verifying the feasibility of the DSSR combustor design for final prototype fabrication.

## ACKNOWLEDGMENTS

Fairchild Stratos Division, Manhattan Beach, California, is the primary contractor in the DSSR program and their participation in the fabrication and assembly of the test apparatus, and test planning and conduct is gratefully acknowledged. In particular, the cooperation and assistance of Messrs. Richard Haglund and Ken Parish are noted. The combustor design was developed by the Institute of Gas Technology, Chicago, Illinois, which also participated in test planning. Mr John W. Stearns, Jr., was the task manager at JPL.

This work was sponsored by the U.S. Department of Energy through an interagency agreement with the National Aeronautics and Space Administration (Task RD 152, Amendment 126, DE-AI01-81ET20307).

## CONTENTS

Tables

# SECTION I

# INTRODUCTION

This document presents results of the combustor test program for the Fairchild Dish Stirling Solar Receiver (DSSR). The purpose of this test program was to evaluate and verify the operational and energy transfer characteristics of the proposed design for combustion augmentation in a hybrid solar receiver utilizing a Stirling engine. The test program was conducted from November 1979 to December 1980 at the Fairchild Stratos Division, Manhattan Beach, California. The DSSR program is supported by the Department of Energy and managed by the Jet Propulsion Laboratory's Advanced Solar Thermal Technology Group of the Thermal Power Systems Project. Fairchild Stratos Division (FSD) is the primary contractor for the DSSR program and the Institute of Gas Technology (IGT) was subcontractor for combustor design.

The purpose of the DSSR program is to demonstrate the technology for a non-heat pipe Dish Stirling Solar Receiver with fossil fuel augmentation[1,2]. This would allow a P-40 United Stirling engine to be operated at constant power and speed under varying solar insolation levels. A diagram of the receiver system is provided in Figure 1. The DSSR is designed to operate on a point-focusing solar concentrator at a solar input of 76.5 $kW_t$. Maximum fossil fuel combustor input would be 67 $kW_t$ with a 10:1 combustor turndown ratio required. The receiver is designed to operate in the hybrid (combustion) mode at all times, where combustor heat input will be at the maximum for zero solar input and the minimum ($\sim$10% max.) at maximum solar input. Solar energy is transferred to the cylinder-side of the 48 Stirling heater tubes which are embedded in the receiver body; energy is transferred

to the regenerator-side of the heater tubes by combustion gases provided by eight burner jets located circumferentially behind the receiver body. Thermal energy thus transferred is converted to shaft power by the Stirling engine, and thence to electricity by a generator.

The objectives of the Combustor Test Program (CTP) were to: (1) verify the ability to start (ignite) without air preheat, control firing rate from minimum to maximum output (with preheat) and vice versa, and shut down the combustor while operating at 10% excess stoichiometric air with natural gas; (2) verify operation of the fuel safety system; (3) verify turndown capability and stability of combustor operation at 10% excess air; and (4) analyze and verify the heat transfer characteristics of the combustor/heat exchanger system.

## SECTION II

## DSSR COMBUSTOR AND HEAT EXCHANGER

The combustor is designed to deliver up to 67 $kW_t$ to the Stirling engine utilizing natural gas as the fuel. The eight burner jets are located circumferentially around the heat exchanger bank (Figure 2). The jets fire tangentially into the annulus behind the heater bank at a maximum outlet velocity of approximately 30 m/sec (100 ft/sec). They are designed to operate at 10% excess stoichiometric air at total flow rates up to 60 g/s (air + fuel). The air is preheated to 1030 K by a recuperator which would provide combustion gas temperatures of 2250 K assuming 20% flame losses. A burner detail is shown in Figure 3.

The heat exchanger bank consists of 48 1.3 cm (0.512 in.) outside diameter (d) tubes with a transverse pitch (s) of 1.41 cm (0.555 in.). The tube bank forms the frustrum of a cone with the smaller diameter of 27.9 cm (11 in.) and larger diameter of 40.6 cm (16 in.). The tubes swirl (or curve) through an arc of approximately 60° from minimum to maximum diameter such that the gap between tubes remains constant at 1.1 mm (0.043 in.) over the surface of the tube bank. A photograph of the tube bank utilized in the combustor test program is presented in Figure 4; and a diagram showing relative tube diameter and spacing is given in Figure 5. For the present application, Stirling engine tube-wall and working fluid (helium) operating temperatures will be approximately 1300 K. Thus for combustion gas temperatures of 2250 K, an average gas-to-tube heat transfer coefficient of approximately 220 $W/m^2$ K (39 $BTU/hr \cdot ft^2 \cdot °F$) is required to transfer 67 $kW_t$ to the working fluid.

Fuel ignition is initially achieved utilizing spark igniters at the outlet of two of the jets. These igniters are also sensors whereby the fuel flow is automatically shut off if the flame extinguishes. Thus, for given combustion

thermal requirements, metered air and fuel flows are supplied to the burner jets, premixed in the jet nozzle, and combusted (see the arrows in Figure 1). The combustion gases enter the annular region, swirl around the tube bank, pass over the tubes and through the tube gaps, heating the Stirling working fluid (helium). Once past the tube bank, the combustion gases will transfer some additional heat to the receiver body and then flow out through the gap behind the receiver body and enter the air preheater. The final products are exhausted to the atmosphere at approximately 650 K.

A complete description of the DSSR, including detailed drawings may be found in Reference 2.

## SECTION III

## DESIGN BACKGROUND

The combustor and heat exchanger system design utilized in the DSSR is based on the geometric configuration, total working fluid volume and thermal input requirements of the United Stirling P-40 engine. The eight-burner combustor was designed to provide uniform combustion gases with a large swirl component, where estimates of flow characteristics for design purposes have been made utilizing potential flow theory. The flow field was assumed to be a sink superimposed upon a vortex for which the velocity potential and stream function for the irrotational, two-dimensional flow are:

$$\phi = -\frac{\dot{V}}{2\pi\ell}\ln r + \Gamma\theta/2\pi, \text{ and} \tag{1a}$$

$$\psi = -\frac{\dot{V}\theta}{2\pi\ell} - \frac{\Gamma}{2\pi}\ln r . \tag{1b}$$

The resulting streamlines are spiral, and the tangent of the angle ($\beta$) between the flow and radial directions is:

$$\tan\beta = \frac{v_\theta}{v_r} = \frac{\Gamma\ell}{\dot{V}} \tag{2}$$

For the present configuration, the vortex strength ($\Gamma$) was evaluated by using the burner outlet jet velocity. To obtain a conservative estimate, $\Gamma$ was then reduced by approximately one-half to account for the finite number of jets and friction losses. The resulting swirl angle ($\beta$) is 76°; and if the vortex strength were again reduced by one-half the resulting $\beta = 64°$. Thus, the estimated swirl angle of incidence upstream of the tube bank is large as indicated in Figure 5; and $\beta$ is relatively insensitive to the assumed vortex strength ($\Gamma$). Also, if the streamlines are determined from equation (1b), it can be shown that the flow traverses approximately one-fourth (90°) of the combustor

circumference prior to entering the tube bank. This should allow adequate mixing of the combustion products for uniform heat transfer to the tube bank.

The DSSR heat exchanger consists of a single row of closely spaced curved tubes in a swirling cross flow as described previously. It is thus a special case of the general category of tubular heat exchangers in cross flow. This category of heat exchangers is widely used in industry and experimental data are available for a range of conditions and configurations. A review of such data is provided by McAdams[3], and later data are provided by Kays and London[4], and Zukauskas[5]. In general, data have been obtained for banks of straight tubes containing several rows that are perpendicular to the direction of cross flow. Local and average convective heat transfer coefficients are determined for different transverse and longitudinal tube spacings. The results are usually correlated with a Reynolds number referenced to tube or hydraulic diameter and flow velocity in the minimum[3, 4, 5] or average[6, 7] free cross-sectional area. For small spanwise spacing ($s/d < 1.25$), empirically determined reference velocities have also been suggested[6].

For single rows of tubes less data are available; the work of Ward and Jewad[6] being an important exception. Those authors[6] reported measurements of heat transfer to a flowing air stream from a single electrically heated tube in a row of closely spaced tubes. The tubes were straight and aligned perpendicular to the flow, where average and local heat transfer coefficients are presented for a range of transverse tube spacings ($1.083 \leq s/d \leq 1.377$). Average Nusselt numbers are correlated with Reynolds numbers based upon velocity in the average free cross-sectional area. For the smallest tube spacings ($s/d \leq 1.176$) an empirically determined reference velocity is employed. The data span a range of Reynolds numbers from approximately $10^3$ to $2 \times 10^4$. However, these data do not completely cover the Reynolds number

range of interest in this investigation and no data are available in the literature for the complex flow geometries studied in this program. Also, previous investigations have usually been conducted with gas-to-tube wall $\Delta T$'s of 10-20 K, while in the present application corresponding $\Delta T$'s are of the order of 1000 K.

Thus, the DSSR heat exchanger performance required further detailed experimental evaluation and analysis prior to final design approval. The foregoing experimental program was designed to meet this need, as well as the other stated objectives.

## SECTION IV

## EXPERIMENTAL SETUP

The combustor test program was conducted utilizing the modified DSSR design shown in Figure 6 without a Stirling engine. The test rig combustor utilizing natural gas and combustion gas heat exchanger configuration is identical to the actual DSSR design. The heat transfer fluid utilized in the test program is water which enters the inlet manifold and flows through the 48 heat exchanger tubes. The tubes extend through a blank receiver body to the outlet manifold where the water flows out. The combustor body is fabricated from a refractory material and the heat exchanger tubes from 310 stainless steel; the tube wall thickness is 0.47 cm (0.184 in.). Combustion air was supplied by a compressed air system and was preheated electrically upstream of the burner jets. The combustion products were exhausted directly to the atmosphere since no recuperator was incorporated in the test rig. Also, the water utilized as the heat transfer fluid was preheated to prevent condensation of water vapor from the combustion products on the tube walls.

Temperature measurements used in heat transfer calculations include: inlet and outlet manifold water temperatures; local water temperatures in the tubes; local tube surface temperatures; combustion gas temperatures; and exhaust product gas temperature. The local water and tube wall temperatures were measured along two tubes as shown in Figure 7, where one tube was located midway between burners and the second located nine tubes in a counterclockwise direction away from the first. Supplemental water temperatures were measured at the inlet and outlet of two tubes located 180° away from the primary (instrumented) tubes. Flame temperatures were measured at two positions in the combustor. Also, receiver body surface temperature was monitored to

insure materials' integrity (Figure 7). Chromel alumel (type K) thermocouples were utilized for temperature measurements, except for combustion gas (flame) temperatures where Platinum vs Platinum-10% Rhodium (Type R) thermocouples were used.

Product (exhaust) gas compositions were monitored continuously to insure that correct air/fuel ratios were maintained and complete combustion occurred. These measurements consisted of: (i) oxygen concentration, and (ii) percent combustibles equivalent to a mixture of equal parts hydrogen and carbon monoxide. Also, the total pressure drop through the combustor was measured by a water manometer.

# SECTION V

# TEST PROGRAM

The combustor test program consisted of three major phases.

Phase 1 - Cold Ignition Performance and Initial Start-Up. The purpose of this phase was to determine the cold ignition criteria for the DSSR combustor. Air/fuel ratios would be established for satisfactory cold-ignition performance. After ignition was established, the firing rate was varied over the design range of operating conditions with cold combustion air, so that the system could be checked out with regard to: safe materials' temperatures; air and fuel flow system operation; heat exchanger water flow system operation; and fuel safety shutoff system performance.

Phase 2 - Turndown Performance. The purpose of this phase was to verify the ability to operate the combustor over the design operating range (10-100%). Specifically, it was necessary to determine whether or not the present burner design could be operated over the firing range of interest with 10% excess air, while maintaining stable flame conditions and satisfactory combustion efficiencies.

Phase 3 - Heat Transfer Characteristics. The purpose of this phase was to analyze in detail the heat transfer characteristics of the combustor in order to determine the ability of the heat exchanger to meet design specifications. The combustor was tested over the design operating range (10-100%) at various combustion air preheat temperatures and with no air preheat. Data obtained in this phase would also add to the technology base for heat exchanger systems of the type studied here.

## SECTION VI

## RESULTS AND DISCUSSION

The results of the Combustor Test Program are presented here for each of the three phases followed by general comments. The results show that the feasibility of the combustor design has been successfully demonstrated for the prototype DSSR.

Phase 1

Cold start ignition was successfully demonstrated at 10% design maximum firing rate. This condition was established with 10% excess combustion air that was not preheated.

The fuel safety shutoff system did not perform satisfactorily. Sensor response to the combustion products during stable operation was intermittent, thus causing interruptions and eventual shutoff of fuel flow unnecessarily. It was thus concluded that greater sensitivity in the ignitor/sensor system would be required. As a result, a three ignitor/probe system with enhanced sensitivity was recommended by the manufacturer, and this system will be employed in the final prototype. Subsequent acceptance testing of the final combustor unit has successfully demonstrated satisfactory operation of the improved fuel safety shutoff system.[2]

All other test systems operated satisfactorily and safe materials temperatures were maintained.

Phase 2

Combustion is stable over the range of operating conditions from 10% to 100% (of design maximum fuel and air input) for air and fuel mixtures in the range of 10% - 13% excess air. This conclusion also applies to operating conditions where there is no combustion air preheat. Measured combustibles in the exhaust products for these conditions were generally less than 0.1%.

Thus, it appears that the DSSR combustor may be operated at a constant air/fuel ratio over the complete range of anticipated operating conditions without loss in combustion efficiency or stability.

Phase 3

Summaries of experimental conditions and combustor performance are presented in Table I for preheated combustion air and in Table II for non-preheated combustion air. A more detailed heat transfer analysis appears in Figures 8 and 9 for tests run with preheated combustion air. Average gas side heat transfer coefficients ($\overline{H}$) were calculated based on total heat transferred to the tube bank, total tube bank surface area of 0.318 $m^2$, and temperature difference, $T_c - \overline{T}_s$. Gas temperatures, $T_c$, were taken to be the average of the two combustion gas thermocouples. Characteristic tube surface temperatures ($\overline{T}_s$) were taken to be an average of the local measurements (Figure 7). This temperature ($\overline{T}_s$) varied from the (extrapolated) temperature at the midpoint of the tube by less than approximately 15 K. To calculate the average heat transfer coefficients along the length of the tube ($\overline{h}$), local water temperature differences and tube surface temperatures were utilized as indicated in Figure 7. The data for each point along the length of the tube in Figure 9 represent an average of measurements from the four instrumented tubes in the heat exchanger. The tube surface and water temperatures utilized in these calculations are tabulated in the Appendix in addition to other miscellaneous data obtained during the test program. Uncertainty of the resulting Nusselt number data based on the average gas side heat transfer coefficient is within ±8% at the highest firing rates and ±12% at the lower firing rates.

During the experiments, outlet bulk-water temperatures were maintained below the saturation temperatures, even at the highest heat transfer rate, so

that the energy transferred to the water increased its measurable sensible heat. At firing rates of 40% and higher, average tube wall inner-surface temperatures, determined from the heat conduction equation by using the measured tube wall outer-surface temperatures and the total heat transferred to each tube, were above the saturation temperature of water. Undoubtedly some surface boiling occurred, but subsequent condensation took place because of the significant amount of water subcooling. Good mixing occurred in the straight tubes and manifold section (Figure 6) between the heater tubes outlets and the location in the manifold outlet where water temperatures were measured. Because of the presence of the thermocouples in the water flow, mixing was also improved in the flow through those heater tubes which were instrumented with water thermocouples, and for which semi-local gas side heat transfer coefficients were determined.

In the present data, Reynolds number is based on the maximum velocity in the minimum free area between tubes and is calculated using the definitions:

$$Re_{max} = \frac{(G_{max})d}{\mu_f} \quad , \tag{3}$$

and

$$G_{max} = \frac{\dot{m}}{A_f} \frac{s}{(s-d)} \quad , \tag{4}$$

where $\dot{m}$ is the total mass flow rate and $A_f$ is the frontal area of the tube bank. Film temperatures for Reynolds and Nusselt $\left(\frac{\bar{H}d}{k_f}\right)$ numbers were taken to be the midpoint between the combustion gas and tube surface temperatures; and transport properties for nitrogen were used. Regarding transport properties, the viscosity of the actual gas mixture was estimated by the technique of

Andrussow[8] and variations from the viscosity of pure nitrogen were found to be less than 5% for the temperature range of interest. Also, the heat transfer coefficients reported here include a radiation component. However, estimates of the contribution of radiation from the refractory to the tube bank have been carried out and the results show that radiation contributes less than 5% of the heat transfer at the highest firing rates and up to 10% of the heat transfer at the lowest firing rates. Radiation from the combustion gases to the tube bank was estimated to be negligible in comparison.

Figure 8 presents heat transfer data for the four air preheat conditions and the range of Reynolds number (firing rates) studied. The data are well correlated by the relation:

$$\overline{Nu} = 0.42\ (Re_{max})^{0.6}\ Pr^{1/3} \qquad (5)$$

which is indicated by the solid line on the figure. Also shown are data from Ward and Jewad[6] for a range of tube spacings. Note that the Ward and Jewad data have been adjusted to account for the different reference velocity used in calculating Reynolds number, the result being a near overlap of the two sets of data at the higher Reynolds numbers. As indicated, the present data show significantly enhanced heat transfer characteristics for the DSSR heat exchanger tube bank when compared to the trend of the data for a perpendicular row of straight tubes, i.e., $\beta = 0$. While part of this enhancement is due to radiation, the majority is presumed due to the large swirl component in the flow which leads to the complex flow pattern incident with the tube bank. In this situation, the superimposed tangential velocity component may act to increase local heat transfer coefficients on the front side of the tubes, thereby increasing the average gas side heat transfer coefficient ($\overline{H}$).

The tubes were also inclined to the flow transversely (Figure 7) and curved (Figure 4) so that the flow field around the tubes was undoubtedly very complex.

Figure 9 shows the variation of heat transfer coefficients along the tube length normalized by the average gas side heat transfer coefficient ($\overline{H}$) and for a range of Reynolds numbers with air preheat. In general, the data show some variations along the length of the tube where the profile exhibiting a peak near the middle was observed most frequently. By referring to Figure 8, the variation of $\overline{h}$ along the tube length can also be interpreted as a variation in local Reynolds number. Thus, these data give an indication of local mass flux nonuniformity along the tube length. This is probably due to flow turning effects near the ends of the tubes at the upper and lower surfaces of the combustor. The extent to which these nonuniformities may affect the performance of the Stirling engine has not yet been analyzed.

The data for tests run with nonpreheated combustion air are given in Table II. Average gas side heat transfer coefficients ($\overline{H}$) are presented for the indicated conditions where the magnitudes of the heat transfer coefficients are seen to be near those observed in the tests with preheated air. However, reduced heat transfer was measured for operating levels greater than 41%. This result is believed due to the loss of a seal during the test cycle and is not considered to be indicative of final combustor performance. As indicated in Table II, the average gas side heat transfer coefficient for the highest operating level (102%) had recovered to within 3% of the maximum $\overline{H}$ measured in preheated air tests.

Insofar as variations around the circumference of the tube bank are concerned, slight nonuniformities were observed. However, while there are not enough data for a detailed analysis, it appears that such variations are not operationally significant.

Finally, utilizing the data in Figure 8, combustor performance for the actual operating conditions of the Stirling engine can be estimated. Operating at the design 100% (maximum) firing rate with P-40 engine tube wall temperatures of approximately 1300K, and assuming combustion gas temperatures of 2150K, the resulting heat transfer coefficient ($\bar{H}$) would be 248 $W/m^2K$ (44 BTU/ $hr \cdot ft^2 \cdot °F$) and total energy transfer would be approximately 67 $kW_t$. Thus it appears that design specifications can be met with the present OSSR combustor/ heat exchanger configuration. Also, a preliminary estimate of overall combustor efficiency indicates that efficiencies in the range of 60-70% may be expected in the final prototype for the stated operating conditions and range of firing rates. Approximately one-half of the estimated losses are due to the air preheater design which exhausts the combustion products to the atmosphere at ≈ 650 K.

General Comments

Measured combustion gas (flame) temperatures were less than the predicted temperature (2250K) which was calculated assuming 20% (flame) heat losses. Thus, combustor heat losses are apparently greater than 20% which may be due to (i) convective heat transfer to the refractory and thence to the surrounds, or (ii) losses associated with system air leakage.

Substantial combustor system air leakage was detected during the conduct of the test program. Consequently, the oxygen concentration was monitored in the combustion products immediately downstream of the heat exchanger tube bank in order to insure that the intended fuel/air ratios were maintained during testing. The flow rate across the heat exchanger was then determined from the known fuel flow rate, measured excess oxygen in the final products and stoichiometry. Air leakage rates upstream of the burner were estimated by subtracting the calculated air flow into the combustor from the measured total air flow to the test rig. Estimated air leakage rates were 15-40% of

total input for the combustor test rig. Final prototype design and assembly should provide for a substantial reduction in system leakage. This will insure correct fuel/air mixtures and thus optimize combustion gas temperatures.

The maximum pressure drop measured through the combustor test rig was 7 inches water column.

There is a potential problem with noise generated by the combustor. In the original design configuration, the noise levels generated during combustor testing were extremely high. Noise levels were subsequently reduced to an "acceptable" level by raising the receiver body one-half inch above the original design position. However, when the plate was again lowered (from the highest position) 3/8 inch, the noise level increased to the previous unacceptable levels. Therefore, the noise is sensitive to the plate location and thus to the geometry and fluid mechanics of the system. The final design location for the receiver body was specified to be at the location where acceptable noise levels were observed. However, it was recommended that the receiver combustor system be tested in as complete a configuration as practicable to insure acceptable operation (in terms of noise level) prior to shipment to United Stirling Sweden.

Instrumentation recommended to monitor combustor operation in the final prototype should include: combustion gas temperature (1); combustion air temperatures before and after the preheater (2); tube wall temperatures on four (4) tubes; flue gas temperatures (2) before and after the preheater; receiver cone temperatures (4) and flue gas analysis.

# SECTION VII

# CONCLUSIONS

An experimental program to evaluate and verify the operational and energy transfer characteristics of the Dish Stirling Solar Receiver (DSSR) combustor and heat exchanger system has been conducted. The combustor/heat exchanger design is characterized by a single row of closely spaced curved tubes in a swirling cross flow of high temperature combustion gases provided by eight burner jets. The results of the program have successfully verified the ability of the system to meet design specifications for the prototype DSSR. Specific conclusions are:

(i) Cold start ignition can be achieved at 10% design maximum firing rate with nonpreheated 10% excess combustion air.

(ii) A two (2) igniter/probe fuel safety system was inadequate and a three (3) igniter/probe system was successfully incorporated.

(iii) The combustor can be controlled adequately and safely, and operated at a constant air/fuel ratio (10% excess air) over the entire range of anticipated firing rates.

(iv) Substantial combustor system air leakages were observed that must be minimized in the final DSSR prototype.

(v) Combustion gas temperatures were lower than expected. A reduction of system air leakages and installation of the air recuperator should provide improvement in this regard.

(vi) Average gas side heat transfer coefficients and semi-local heat transfer coefficients along the lengths of the tubes were obtained. The results show significantly enhanced heat transfer characteristics for the DSSR heat exchanger when compared to similar data for closely spaced tubes perpendicular to cross flow. These data provide new information on heat transfer

to tubes in cross flow that can be achieved in a high temperature combustion system when complex geometries such as the one described here are utilized. Furthermore, it was concluded that the present DSSR combustor/heat exchanger met design thermal requirements such that prototype fabrication could proceed.

## REFERENCES


1. Haglund, R. and Tatge, R. "Dish Stirling Solar Receiver (DSSR)," 3rd Semi-Annual Advanced Technology Meeting: A Review of Advanced Solar Thermal Power Systems (Meeting Abstracts), at Long Beach, CA, U.S. Department of Energy, pp. 20-28, June 1979.

2. Haglund, R. and Burns, J.R., "Dish Stirling Solar Receiver Program Final Report", Document No. ER 79917-3, Contract No. 455400, Fairchild Stratos Division, Manhattan Beach, CA, December 1980.

3. McAdams, W.H., Heat Transmission, 3rd Edition, McGraw Hill, NY, NY, pp. 258-276, 1954.

4. Kays, W.M. and London, A.L., Compact Heat Exchangers, 2nd ed., McGraw Hill, New York, Chapters 7 and 10, 1964.

5. Zukauskas, A., "Heat Transfer from Tubes in Cross Flow", in Advances in Heat Transfer, Volume 8, ed. by J.P. Hartnett and T.F. Irvine, Jr., Academic Press, NY, NY, pp. 93-160, 1972.

6. Ward, J. and Jewad, M.A., "Local and Average Heat Transfer Associated With a Single Row of Closely-Spaced Tubes in Cross Flow", Heat Transfer 1978, Vol. 4, National Research Council of Canada, Toronto, pp. 273-278, 1978.

7. Perkins, H.C., Jr. and Leppert, G., "Forced Convection Heat Transfer From a Uniformly Heated Cylinder", Journal of Heat Transfer, Vol. 84, pp. 257-263, 1962.

8. Andrussow, L., "Diffusion, Viscosity and Conductivity of Gases", Progress in International Research on Thermodynamic and Transport Properties, ed. by J.F. Masi and D.H. Tsai, American Society of Mechanical Engineers, Academic Press, NY, NY, pp. 279-287, 1962.

## NOMENCLATURE

$A_f$ = frontal area of the tube bank

$d$ = outside tube diameter

$G_{max}$ = mass flow rate per unit area in the minimum free area between tubes

$\bar{h}$ = local average heat transfer coefficient along the tube length based on $(\bar{T}_c - T_{s_n})$

$\bar{H}$ = average gas side heat transfer coefficient to heater tubes based on $(T_c - \bar{T}_s)$

$k_f$ = gas film thermal conductivity

$\ell$ = combustion chamber height

$\dot{m}$ = total mass flow rate

$\overline{Nu}$ = Nusselt number, $\bar{H}d/k_f$

$Pr$ = gas film Prandtl number

$\dot{Q}_F$ = total energy supplied by the fuel

$\dot{Q}_W$ = total heat transfer rate to water flow through tubes

$r$ = radius of combustion chamber cross-section

$Re_{max}$ = Reynolds number based on maximum velocity in the minimum free area between tubes and tube outside diameter, $G_{max}d/\mu_f$

$s$ = transverse center-to-center tube spacing (pitch)

$T_A$ = temperature of preheated combustion air

$T_B$ = receiver body temperature

$T_c$ = combustion gas temperature

$T_p$ = flue gas temperature

$T_{s_n}$ = local tube wall temperature at the $n^{th}$ location along the tube length

$\bar{T}_s$ = average tube wall temperature

$T_{W_i}$ = water temperature in the inlet manifold

$T_{W_o}$ = water temperature in the outlet manifold

$T_{W_n}$ = local water temperature at the $n^{th}$ location along the tube length

$v_r$ = radial velocity component

$v_\theta$ = tangential velocity component

$\dot{V}$ = volumetric flow rate

$\beta$ = angle between the flow and radial directions

$\Gamma$ = vortex strength $\left(\frac{m^2}{s}\right)$

$\theta$ = turning angle in polar coordinates

$\mu_f$ = gas film viscosity

$\phi$ = velocity potential

$\psi$ = stream function

TABLE I

DSSP COMBUSTOR EXPERIMENTAL CONDITIONS

WITH AIR PREHEAT

| Operating level %* | $T_A$ K | Excess Stoichiometric Air % | $\dot{Q}_F$ kW | $\dot{Q}_W$ kW | $\frac{\overline{H}}{W}$ $\frac{W}{m^2K}$ | $T_C$ K | $T_P$ K | $T_S$ K |
|---|---|---|---|---|---|---|---|---|
| 13 | 1035 | 11.75 | 19.0 | 18.7 | 51.0 | 1520 | 530 | 360 |
| 30.4 | 1035 | 11.75 | 44.2 | 36.6 | 91.2 | 1710 | 690 | 450 |
| 40.8 | 1035 | 11.0 | 58.1 | 45.9 | 114 | 1760 | 740 | 490 |
| 50.4 | 975 | 11.75 | 73.4 | 51.9 | 128 | 1810 | 740 | 530 |
| 10 | 810 | 11.75 | 14.5 | 18.5 | 51.4 | 1480 | 500 | 360 |
| 20.1 | 810 | 11.75 | 27.6 | 25.1 | 65.9 | 1590 | 580 | 390 |
| 30 | 810 | 11.75 | 41.3 | 35.6 | 90.7 | 1680 | 660 | 440 |
| 40 | 810 | 11.5 | 55.0 | 45.5 | 113 | 1760 | 740 | 490 |
| 50.4 | 810 | 11.75 | 69.5 | 46.9 | 119 | 1750 | 740 | 500 |
| 63 | 810 | 11.0 | 86.8 | 57.4 | 142 | 1820 | 800 | 540 |
| 71.6 | 810 | 11.75 | 98.6 | 66.0 | 162 | 1860 | 860 | 580 |
| 82.5 | 810 | 13.0 | 113.6 | 73.3 | 181 | 1890 | 930 | 610 |
| 92 | 755 | 11.5 | 126.6 | 78.5 | 198 | 1910 | 960 | 660 |

*Percent of predicted fuel input required with 10% excess air preheated to 1035K for 67 kW input to Stirling engine. Fuel + air mass flow rate at 100% = 55.5g/sec.

TABLE II

DSSR COMBUSTOR EXPERIMENTAL CONDITIONS

WITH NO AIR PREHEAT ($T_A$ = 290K)

| Operating level %* | Excess Stoichiometric Air % | $\dot{Q}_F$ kW | $\dot{Q}_W$ kW | $\frac{\bar{H}}{W}$ $\frac{}{m^2K}$ | $T_c$ K | $T_p$ K | $T_s$ K |
|---|---|---|---|---|---|---|---|
| 10 | 10.0 | 14.5 | 15.1 | 46.0 | 1401 | 508 | 366 |
| 20 | 10.0 | 29.2 | 19.9 | 59.6 | 1444 | 546 | 389 |
| 31.5 | 10.0 | 45.9 | 28.3 | 80.6 | 1534 | 630 | 427 |
| 41.2 | 10.0 | 60.0 | 35.4 | 97.6 | 1614 | 703 | 472 |
| 50.4 | 11.75 | 73.4 | 32.6 | 92.5 | 1599 | 619 | 489 |
| 61.3 | 11.75 | 89.1 | 39.7 | 111 | 1654 | 699 | 527 |
| 71.2 | 10.0 | 103.6 | 46.9 | 130 | 1697 | 760 | 561 |
| 81.5 | 10.0 | 118.5 | 53.5 | 148 | 1731 | 814 | 589 |
| 91.7 | 10.5 | 133.3 | 61.9 | 174 | 1746 | 864 | 627 |
| 102 | 10.0 | 148.6 | 67.8 | 192 | 1757 | 898 | 644 |

*Percent of predicted fuel input required with 10% excess air preheated to 1035K for 67 kW input to Stirling engine. Fuel + air mass flow rate at 100% = 55.5 g/sec.

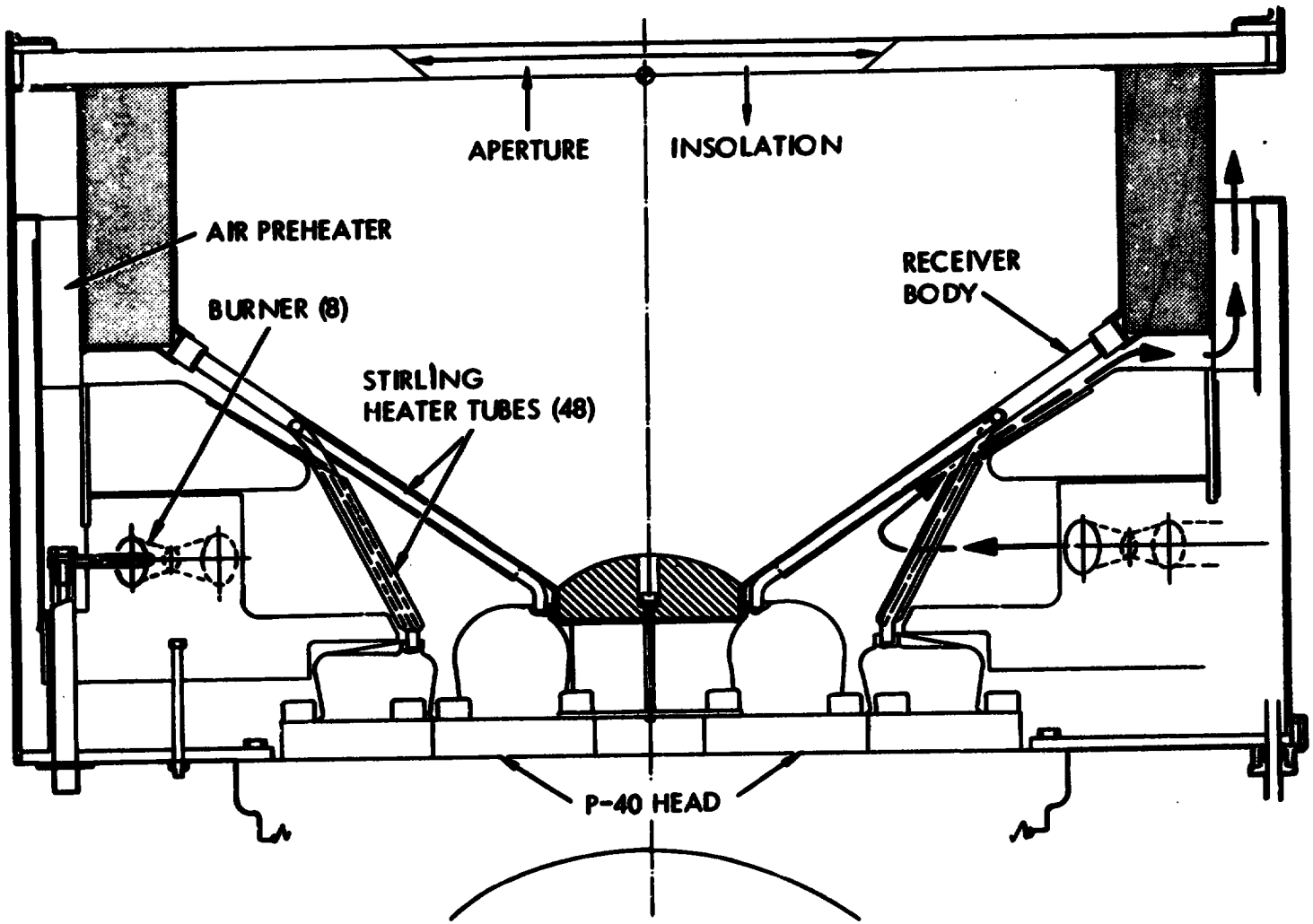


FIGURE 1. DISH STIRLING SOLAR RECEIVER

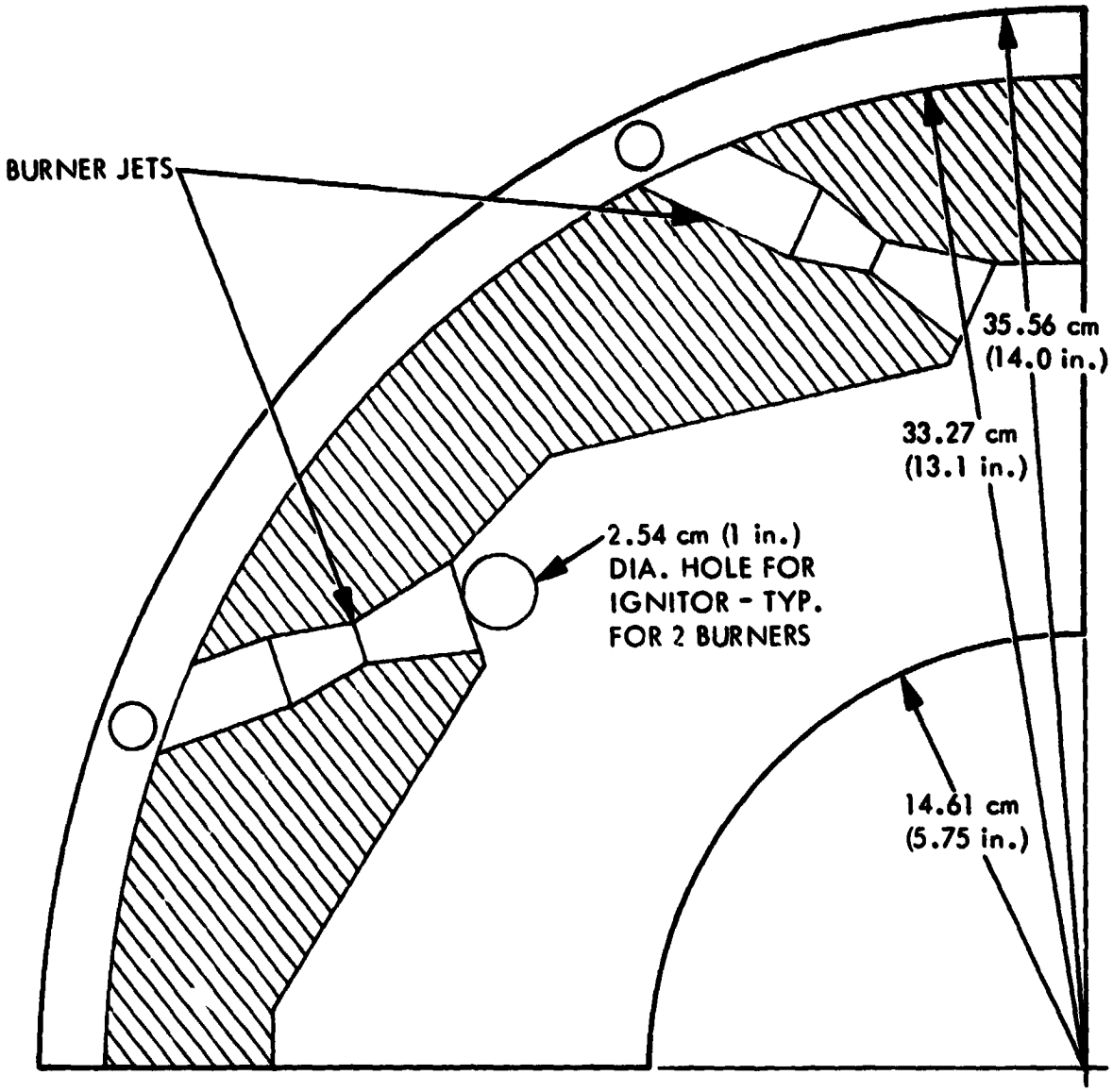


FIGURE 2. COMBUSTOR QUADRANT CROSS-SECTION (PLAN VIEW)

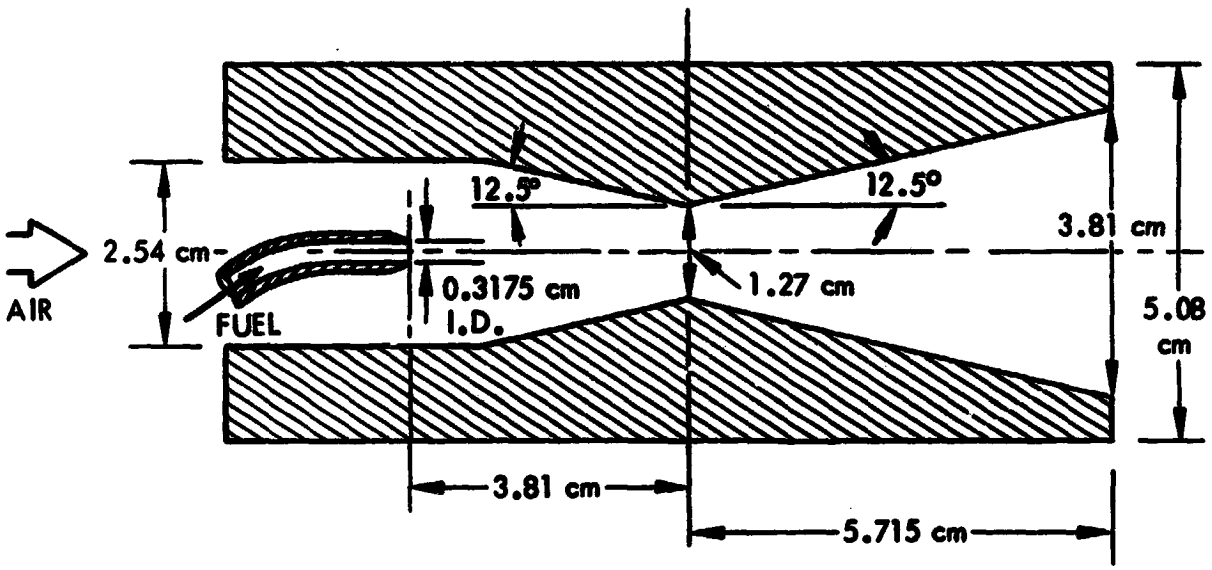


FIGURE 3. BURNER DETAIL

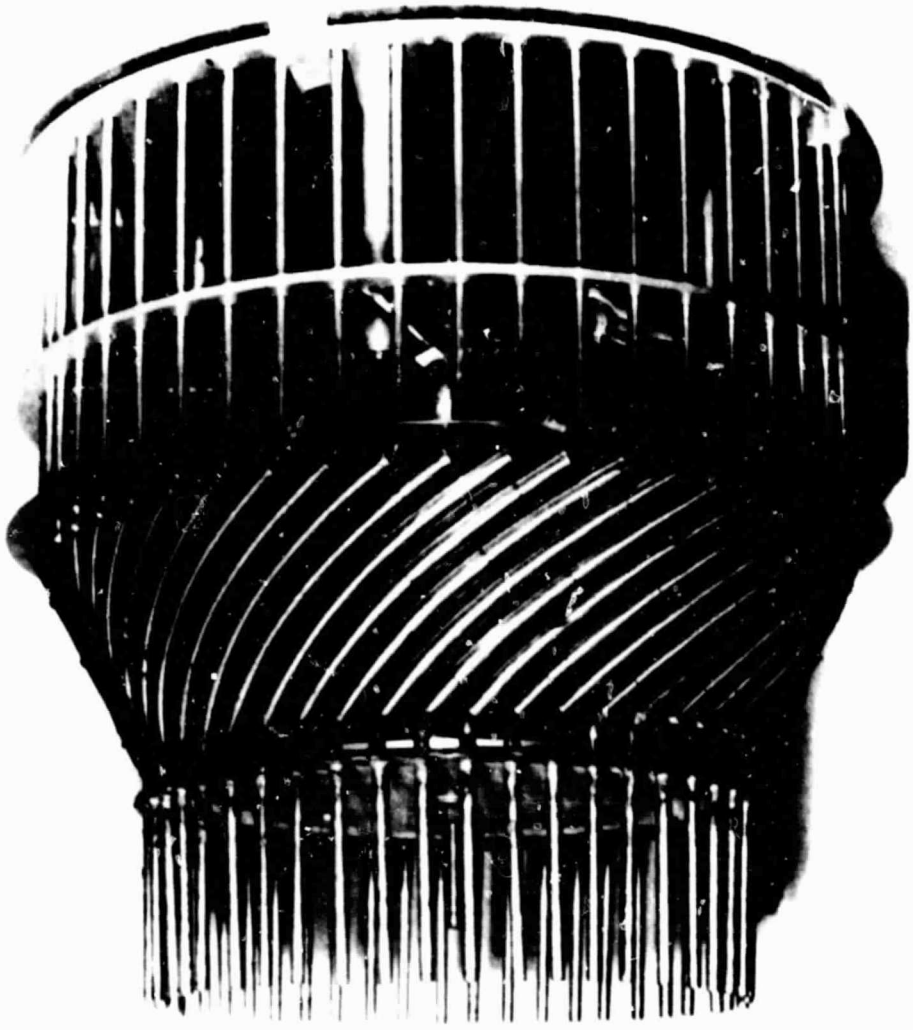

FIGURE 4. COMBUSTOR TEST RIG HEAT EXCHANGER TUBE BANK

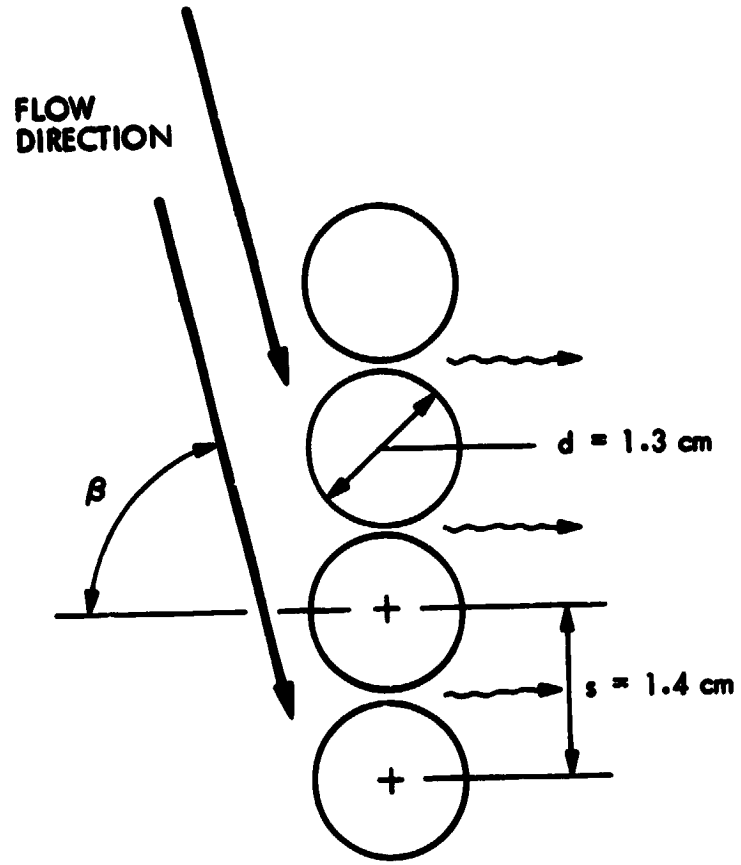


FIGURE 5. TUBE AND FLOW CONFIGURATION

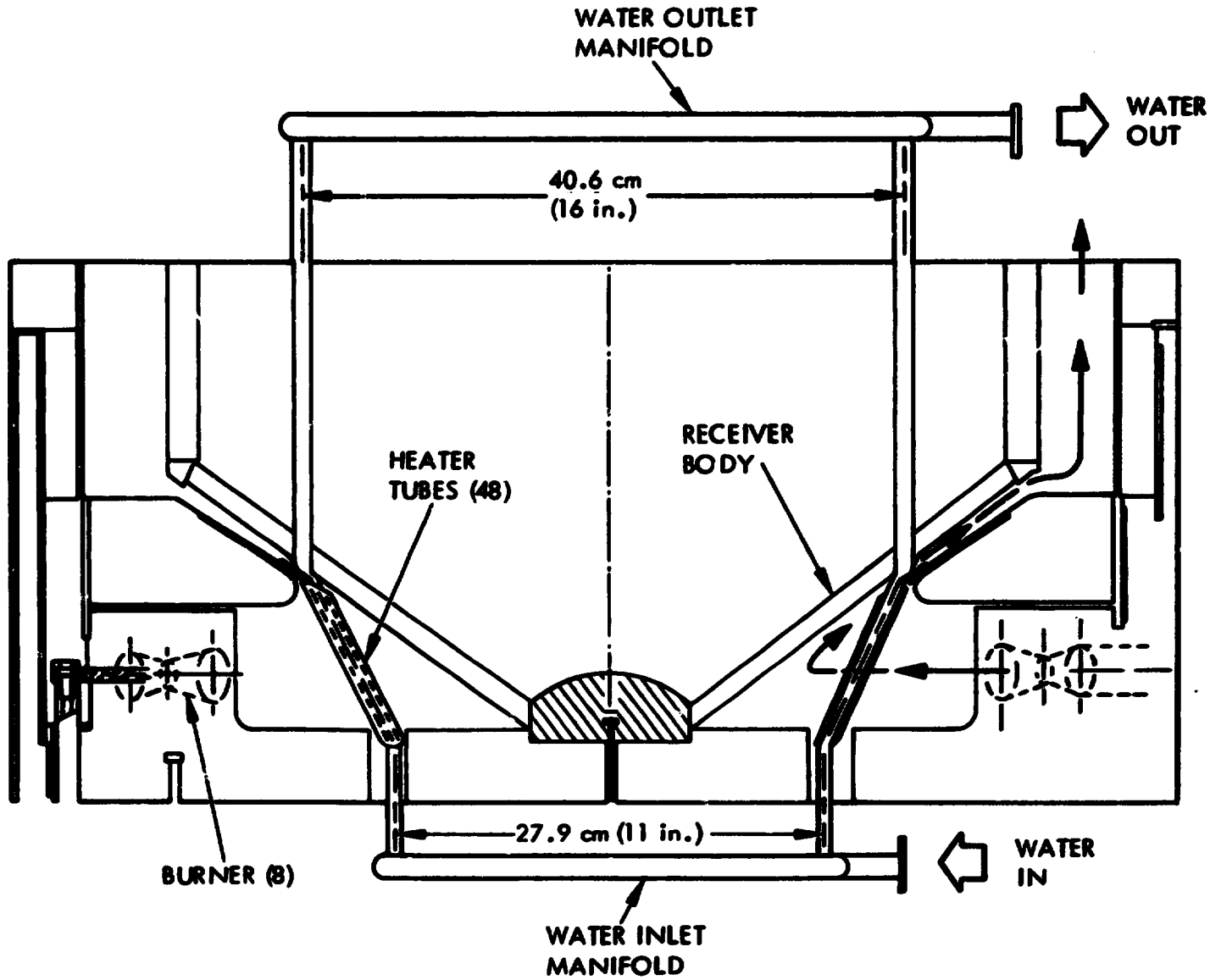


FIGURE 6. DSSR COMBUSTOR TEST RIG

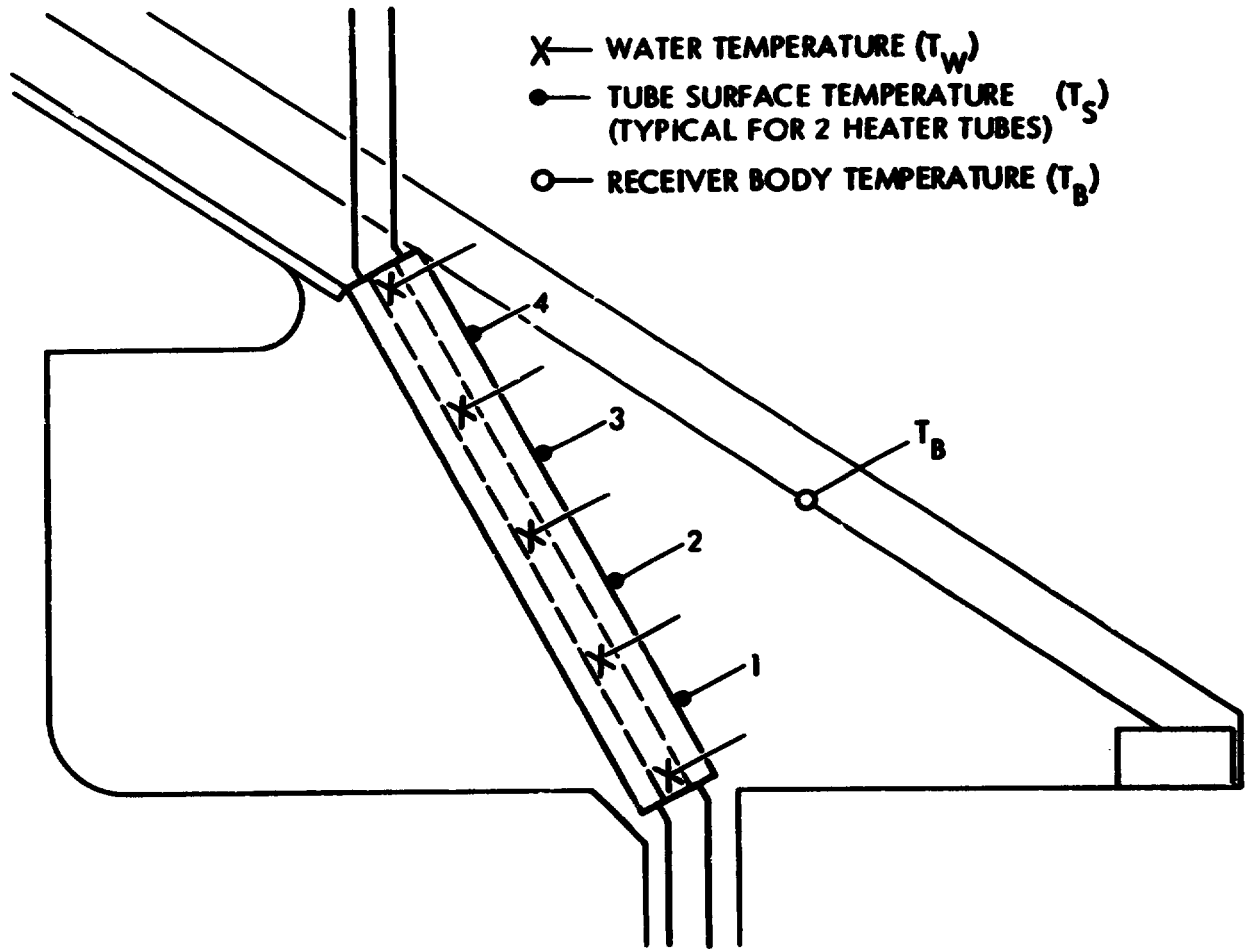


FIGURE 7. DSSR COMBUSTOR HEATER TUBE INSTRUMENTATION

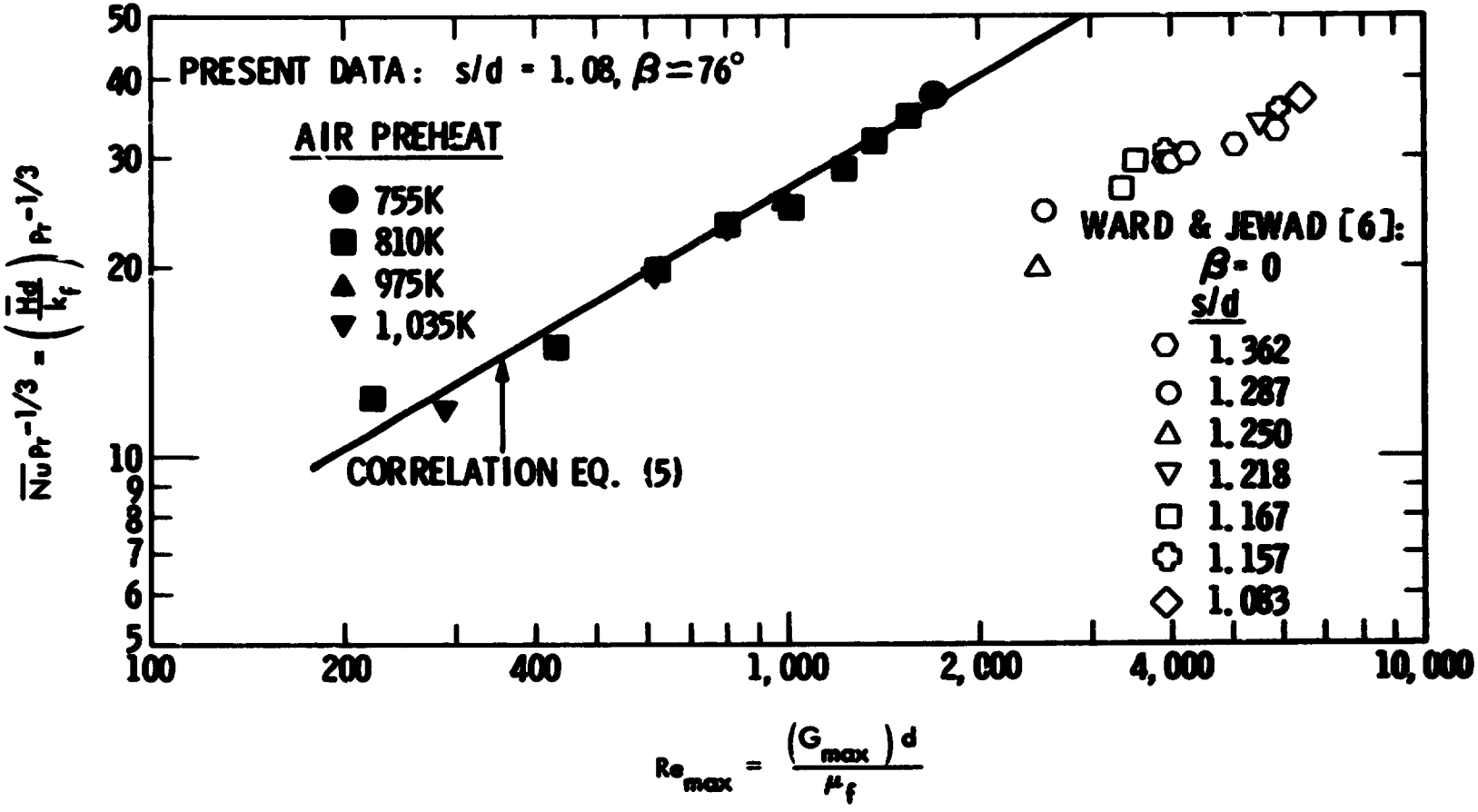


FIGURE 8. AVERAGE GAS SIDE HEAT TRANSFER COEFFICIENTS

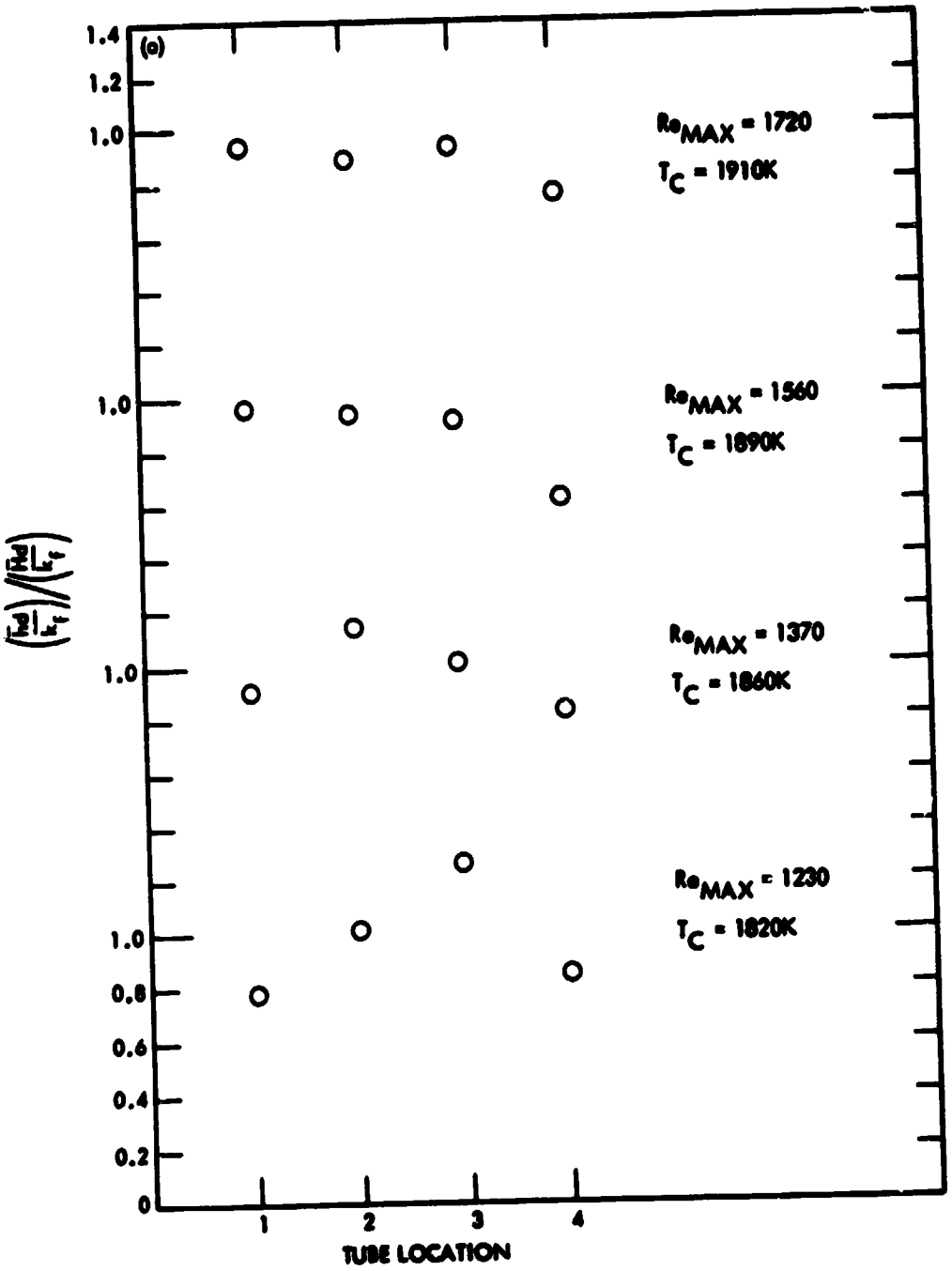


**FIGURE 9. HEAT TRANSFER COEFFICIENTS ALONG THE TUBE LENGTH: (a) $Re_{max}$ = 1230–1720**

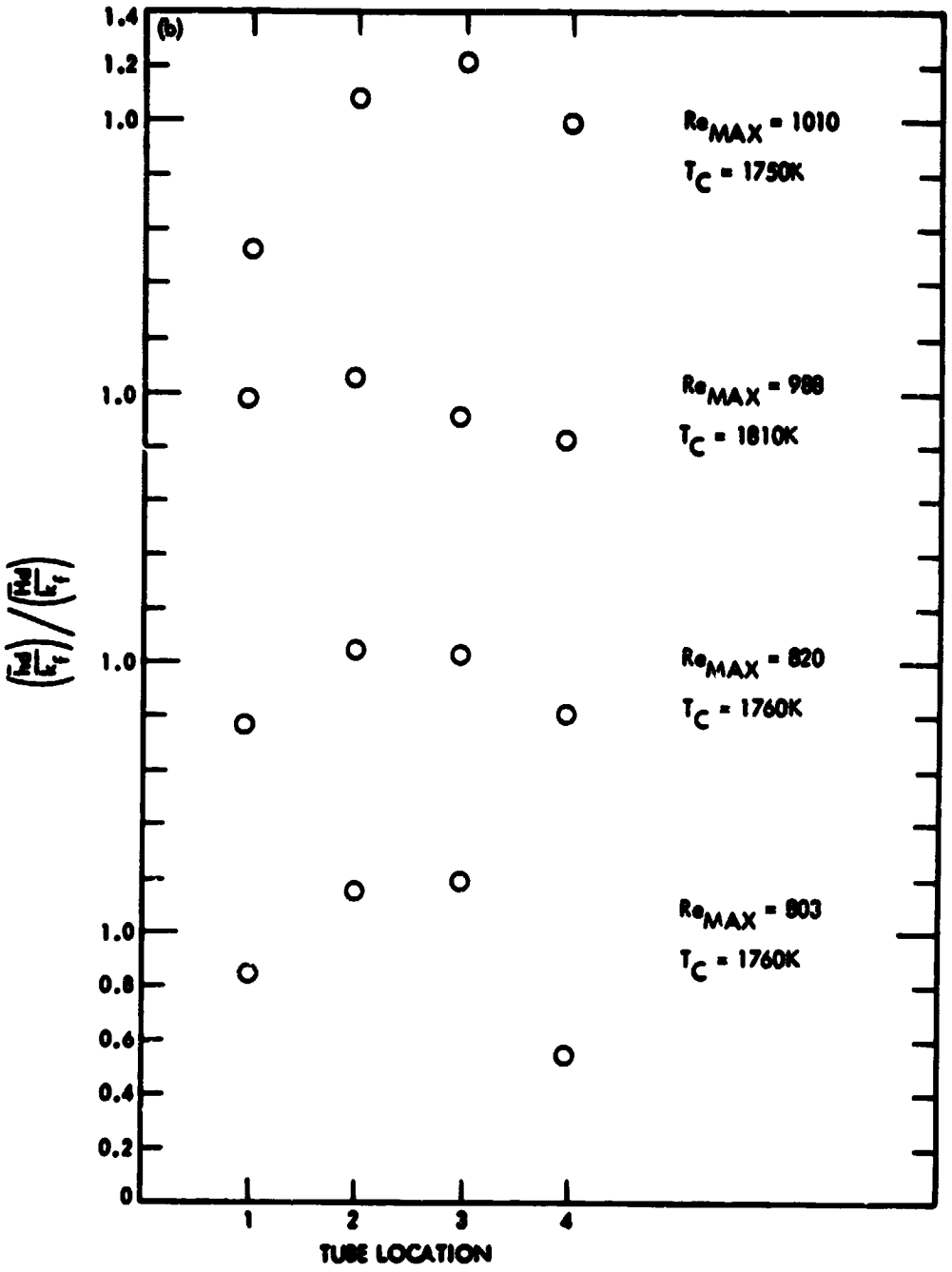


**FIGURE 9. HEAT TRANSFER COEFFICIENTS ALONG THE TUBE LENGTH: (b) $Re_{max}$ = 803-1010**

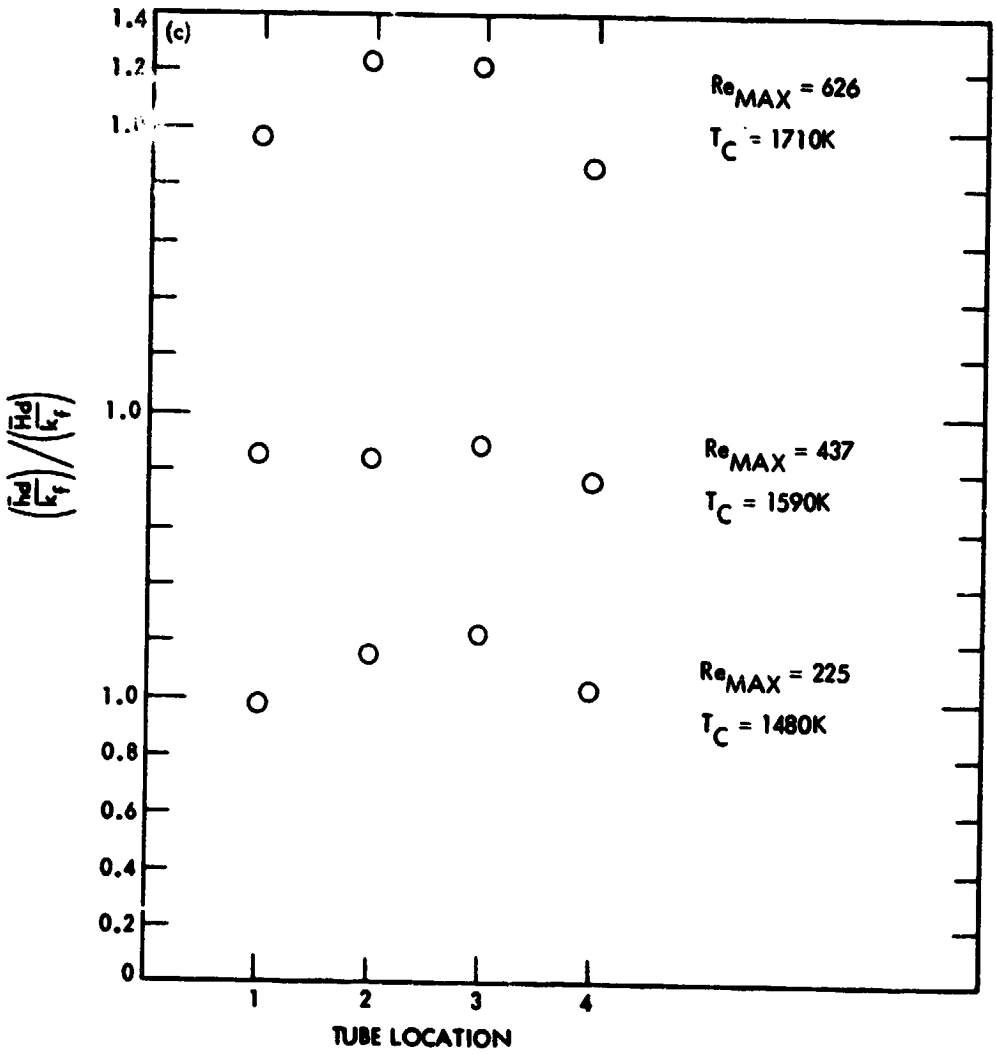


**FIGURE 9. HEAT TRANSFER COEFFICIENTS ALONG THE TUBE LENGTH: (c) $Re_{max}$ = 225–626**

# APPENDIX

# MISCELLANEOUS TABULATED DATA

TABLE A-1

DSSR COMBUSTOR MEASUREMENTS

WITH AIR PREHEAT

| Operating level %* | $T_A$ K | $T_{W_i}$ K | $T_{W_o}$ K | $T_{W_1}$ K | $T_{W_2}$ K | $T_{W_3}$ K | $T_{W_4}$ K | $T_{W_5}$ K | $T_{S_1}$ K | $T_{S_2}$ K | $T_{S_3}$ K | $T_{S_4}$ K | $T_B$ K | Total Water Flow Rate liters/min |
|---|---|---|---|---|---|---|---|---|---|---|---|---|---|---|
| 13 | 1035 | 292 | 308 | 295 | 297 | 299 | 300 | 304 | 327 | 350 | 377 | 400 | 494 | 17.2 |
| 30.4 | 1035 | 296 | 327 | 298 | 304 | 311 | 319 | 324 | 372 | 422 | 475 | 522 | 583 | 17.2 |
| 40.8 | 1035 | 298 | 336 | 302 | 309 | 317 | 325 | 330 | 394 | 461 | 525 | 577 | 612 | 17.2 |
| 50.4 | 975 | 299 | 342 | 304 | 311 | 320 | 329 | 336 | 422 | 494 | 566 | 625 | 636 | 17.2 |
| 10 | 810 | 292 | 307 | 292 | 295 | 299 | 302 | 305 | 314 | 344 | 372 | 394 | 486 | 17.2 |
| 20.1 | 810 | 293 | 314 | 297 | 300 | 304 | 307 | 311 | 341 | 372 | 408 | 439 | 537 | 17.2 |
| 30 | 810 | 295 | 325 | 299 | 303 | 307 | 311 | 317 | 372 | 422 | 469 | 508 | 588 | 17.2 |
| 40 | 810 | 297 | 336 | 301 | 306 | 315 | 325 | 331 | 400 | 466 | 522 | 566 | 649 | 17.2 |
| 50.4 | 810 | 298 | 337 | 303 | 312 | 322 | 330 | 334 | 416 | 489 | 544 | 569 | 639 | 17.2 |
| 63 | 810 | 300 | 349 | 307 | 316 | 329 | 338 | 345 | 444 | 527 | 586 | 616 | 680 | 17.2 |
| 71.6 | 810 | 302 | 358 | 309 | 319 | 331 | 343 | 352 | 461 | 555 | 630 | 675 | 727 | 17.2 |
| 82.5 | 810 | 306 | 369 | 314 | 322 | 334 | 345 | 356 | 483 | 577 | 666 | 730 | 774 | 17.2 |
| 92 | 755 | 307 | 373 | 316 | 327 | 340 | 351 | 362 | 500 | 605 | 716 | 811 | 799 | 17.2 |

*Percent of predicted fuel input required with 10% excess air preheated to 1035K for 67 kW input to Stirling engine. Fuel + air mass flow rate at 100% = 55.5 g/sec.

TABLE A-2

DSSR COMBUSTOR MEASUREMENTS

WITH NON-PREHEATED AIR ($T_A$ = 290K)

| Operating level %* | $T_{W_{K_i}}$ | $T_{W_{K_o}}$ | $T_{W_{K_1}}$ | $T_{W_{K_2}}$ | $T_{W_{K_3}}$ | $T_{W_{K_4}}$ | $T_{W_{K_5}}$ | $T_{S_{K_1}}$ | $T_{S_{K_2}}$ | $T_{S_{K_3}}$ | $T_{S_{K_4}}$ | $T_{B_K}$ | Total Water Flow Rate liters/min |
|---|---|---|---|---|---|---|---|---|---|---|---|---|---|
| 10 | 302 | 313 | 302 | 303 | 304 | 306 | 309 | 327 | 358 | 372 | 380 | 500 | 20.6 |
| 20 | 303 | 317 | 302 | 303 | 305 | 307 | 311 | 333 | 375 | 397 | 414 | 536 | 20.6 |
| 31.5 | 295 | 317 | 298 | 301 | 304 | 310 | 314 | 358 | 408 | 450 | 480 | 611 | 18.7 |
| 41.2 | 297 | 324 | 300 | 302 | 307 | 315 | 321 | 386 | 441 | 497 | 544 | 679 | 18.7 |
| 50.4 | 330 | 351 | 330 | 331 | 334 | 339 | 345 | 391 | 458 | 514 | 547 | 501 | 21.7 |
| 61.3 | 328 | 355 | 330 | 331 | 335 | 340 | 347 | 422 | 494 | 558 | 605 | 572 | 21.2 |
| 71.2 | 330 | 362 | 331 | 334 | 340 | 349 | 357 | 436 | 522 | 597 | 647 | 615 | 21.2 |
| 81.5 | 334 | 371 | 336 | 339 | 345 | 355 | 365 | 458 | 550 | 630 | 694 | 674 | 20.6 |
| 91.7 | 326 | 372 | 334 | 341 | 347 | 357 | 366 | 480 | 577 | 672 | 741 | 722 | 19.5 |
| 102 | 303 | 354 | 306 | 316 | 325 | 337 | 348 | 491 | 594 | 691 | 764 | 744 | 19.3 |

*Percent of predicted fuel input required with 10% excess air preheated to 1035K for 67 kW input to Stirling engine. Fuel + air mass flow rate at 100% = 55.5 g/sec.